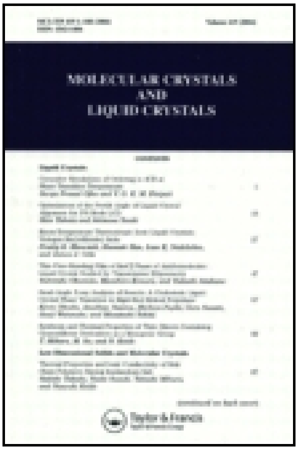

Molecular Crystals and Liquid Crystals Science and Technology. Section A. Molecular Crystals and Liquid Crystals

Publication details, including instructions for authors and subscription information:
http://www.tandfonline.com/loi/gmcl19

Resonant Magnetization Tunneling in Single-Molecule Magnets

Sheila M. J. Aubin [a] , Daniel Ruiz [a] , Evan Rumberger [a] , Ziming Sun [a] , Belen Albela [b] , Michael W. Wemple [c] , Neil R. Dilley [d] , Joan Ribas [b] , M. Brian Maple [d] , George Christou [c] & David N. Hendrickson [a]

[a] Department of Chemistry and Biochemistry-0358, University of California at San Diego, La Jolla, California, 92093-0358, U.S.A

[b] Departament de Quimica Inorganica, Universitat de Barcelona, Diagonal 647, E-08028, Barcelona, Spain

[c] Department of Chemistry, Indiana University, Bloomington, Indiana, 47405-4001, U.S.A

[d] Department of Physics, University of California at San Diego, La Jolla, California, 92093-0358, U.S.A.

To cite this article: Sheila M. J. Aubin, Daniel Ruiz, Evan Rumberger, Ziming Sun, Belen Albela, Michael W. Wemple, Neil R. Dilley, Joan Ribas, M. Brian Maple, George Christou & David N. Hendrickson (1999): Resonant Magnetization Tunneling in Single-Molecule Magnets, Molecular Crystals and Liquid Crystals Science and Technology. Section A. Molecular Crystals and Liquid Crystals, 335:1, 371-389

To link to this article: http://dx.doi.org/10.1080/10587259908028881

Mol. Cryst. and Liq. Cryst., 1999, Vol. 335, pp. 371-389
Reprints available directly from the publisher
Photocopying permitted by license only

Published by license under the
Gordon and Breach Science Publishers imprint.
Printed in Malaysia

Resonant Magnetization Tunneling in Single-Molecule Magnets

SHEILA M. J. AUBIN[a], DANIEL RUIZ[a], EVAN RUMBERGER[a], ZIMING SUN[a], BELEN ALBELA[b], MICHAEL W. WEMPLE[c], NEIL R. DILLEY[d], JOAN RIBAS[b], M. BRIAN MAPLE[d], GEORGE CHRISTOU[c] and DAVID N. HENDRICKSON[a]

[a]*Department of Chemistry and Biochemistry-0358, University of California at San Diego, La Jolla, California 92093–0358, U.S.A,* [b]*Departament de Quimica Inorganica, Universitat de Barcelona, Diagonal 647, E-08028-Barcelona, Spain,* [c]*Department of Chemistry, Indiana University, Bloomington, Indiana 47405–4001, U.S.A and* [d]*Department of Physics, University of California at San Diego, La Jolla, California 92093–0358, U.S.A.*

Data are presented for three different types of single-molecule magnets (SMM's): $[Mn_{12}O_{12}(O_2CR)_{16}(H_2O)_4]$, $[Cation][Mn_{12}O_{12}(O_2CR)_{16}(H_2O)_4]$, and the distorted cubane $[Mn^{IV}Mn^{III}{}_3O_3X(O_2CR)_3L_3]$ complexes. All three types of complexes exhibit slow magnetization relaxation at temperatures below 5 K. Each molecule can change the direction of its magnetization only slowly at these low temperatures. Manisfetations of this are seen in magnetization hysteresis loops and in the presence of frequency-dependent out-of-phase ac magnetic susceptibility signals (χ''_M). It is shown that the neutral Mn_{12} SMM's exist in isomeric forms that differ in the positoning of the 4 H_2O and 16 carboxylate ligands. The orgin of the two χ''_M signals for the neutral Mn_{12} complexes is discussed. All Mn_{12} complexes exhibit magnetization hysteresis loops with steps seen at regular increments of magnetic field. The step heights and coercive fields for the loops vary from one Mn_{12} SMM to another. Step-structured hysteresis loops are also seen for both the $S = 19/2$ $[Mn_{12}^-]$ and $S = 9/2$ $[Mn_4]$ SMM's. The steps seen at zero field are interesting since these are half-integer spin complexes that should not tunnel in zero field. Apparently, an internal magnetic field due to the nuclear spins in the complex is responsible for the tunneling of these half-integer spin complexes.

INTRODUCTION

A single-molecule magnet (SMM) is the ultimate high-density memory device,[1] for each molecule is on the order of 10-20 Å in diameter. SMM's could also be used in quantum computers.[2] Considerable research is directed at studying SMM's in order to elucidate how quantum-mechanical behavior observed in these molecules underlies classical behavior at the macroscopic level.[3]

Each SMM functions as a superparamagnet. The source of the magnetoanisotropy is the molecule's high spin ground state combined with appreciable zero-field splitting. At temperatures below the "blocking temperature" the magnetic moment of a SMM changes sluggishly from spin "up" to spin "down". This slow magnetization relaxation leads to: (1) magnetization hysteresis loops; (2) frequency-dependent out-of-phase ac magnetic susceptibility signals; (3) a divergence between zero-field-cooled and field-cooled magnetization data at the "blocking temperature"; and (4) slow magnetization decay after an external magnetic field is removed when the temperature is below the "blocking temperature". It is important to emphasize that the SMM phenomenon comes from the behavior of individual isolated molecules.[4]

The first and most thoroughly studied[5-25] SMM is $[Mn_{12}O_{12}(O_2CR)_{16}(H_2O)_4]\cdot S$ (complex **1**) where R is $-CH_3$ and S is $4H_2O\cdot 2HO_2CCH_3$. The slow magnetization relaxation for this complex has been shown[10] to be due to a $S = 10$ ground state split by axial zero-field splitting $(D\hat{S}_z^2)$, where $D = -0.50\ \mathrm{cm}^{-1}$. There is a double-well potential-energy curve for reversal of the direction of magnetization for each SMM. The temperature dependence of the rate for reversal of the direction of magnetization of each molecule is well described by the Arrhenius law. The effective activation barrier was found[15] to be smaller than the thermodynamic barrier $U = |D|\hat{S}_z^2 = 72$ K, expected for a $S = 10$ ground state split by zero-field interactions with $D = -0.50\ \mathrm{cm}^{-1}$.

The most interesting finding for the SMM complex **1** was made in 1996.[16-18] It was found that, in addition to thermal activation of each SMM over the barrier, the reversal of the direction of the magnetization also occurs via quantum mechanical tunneling through the barrier. The compelling evidence for resonant magnetization tunneling comes from the observation of steps in the magnetization hysteresis loops occurring at constant intervals of the external magnetic field.[16-18] At the low temperatures (< 2.5 K) of the hysteresis measurements, each molecule interacts with phonons in an Orbach process to be excited incrementally from the $M_s = -10$ level to the $M_s = -9, -8, -7$, etc. level. Calculations for the SMM complex **1** have shown that the most likely pathway for quantum tunneling of the magnetization involves tunneling between the $M_s = \pm 3$ levels in zero field.[16c]

In this paper new results are presented for different SMM's with the compositions of $[Mn_{12}O_{12}(O_2CR)_{16}(H_2O)_4]$, $[\mathrm{Cation}][Mn_{12}O_{12}(O_2CR)_{16}(H_2O)_4]$, and $[Mn^{IV}Mn^{III}_3O_3Cl(O_2CCH_3)_3(dbm)_3]$.

EXPERIMENTAL SECTION

Compound Preparation. Samples of $[Mn_{12}O_{12}(O_2CR)_{16}(H_2O)_4]$ with different R substituents were prepared by replacing the acetate ligands on complex **1**. Complex **1** was synthesized as previously described.[6] A slurry of complex **1** (0.50 g, 0.25 mmol) in CH_2Cl_2 (50 mL) was treated with an excess of the corresponding carboxylic acid RCO_2H (8.0 mmol). The mixture was stirred overnight in a closed flask and filtered to remove any undissolved solid. Hexanes were added to the filtrate until precipitation of a dark brown solid was observed. The resulting solid was collected by filtration and the above treatment was repeated. Recrystallization from CH_2Cl_2/hexanes gave crystals of the various complexes suitable for X-ray structure analyses. All compounds studied gave satisfaactory analytical data.

Physical Measurements. DC magnetic susceptibility data were collected on microcrystalline samples or a single-crystal sample restrained in eicosane to prevent torquing on a Quantum Design MPMS5 SQUID magnetometer equipped with a 5.5 T (55 kOe) magnet. A diamagnetic correction to the observed susceptibilities was applied using Pascal's constants. Alternating current (ac) susceptibility measurements were carried out on a Quantum Design MPMS2 SQUID magnetometer equipped with a 1 T (10 kOe) magnet and capable of achieving temperatures of 1.7 to 400 K. The ac field range is 1×10^{-4} to 5 Oe, oscillating at a frequency in the range of 5×10^{-4} to 1512 Hz. Sample alignments in eicosane were performed while keeping the samples in a 5.5 T field at a temperature above the melting point (308-312 K) of eicosane for 15 min, after which the temperature was gradually decreased below the melting point to solidify the eicosane in order to constrain the sample. In this way we could prepare a wax cube with little crystals oriented in the wax cube.

Magnetization hysteresis loops were collected on either a Faraday magnetometer or a Quantum Design MPMS5 SQUID magnetometer employing oriented single crystals. The crystals were first added to eicosane and torqued in a 55 kOe field.

RESULTS AND DISCUSSION

$[Mn_{12}O_{12}(O_2CR)_{16}(H_2O)_4]$ Single Molecule Magnets. Lis reported[6] the preparation and structure of complex **1** in 1980, where R is $-CH_3$. In 1993 we reported[26] the X-ray structure of the benzoate (R is $-C_6H_5$) complex **2** and then the propionate[4a] (R is $-CH_2CH_3$) complex **3** in 1995. Very recently two new Mn_{12} SMM with R = $-C_6H_4$-2-Cl (complex **4**) and R = C_6H_4-2-Br (complex **5**) were reported.[27] The properties of two isomeric forms of $[Mn_{12}O_{12}(O_2CC_6H_4\text{-}4\text{-}Me)_{16}(H_2O)_4]$ (**6**), complexes **6**·$3H_2O$ and **6**·$HO_2CC_6H_4\text{-}4Me$, were communicated.[28]

All of the above Mn_{12} SMM's have similar molecular structures. As shown in Figure 1, there is a $[Mn_{12}(\mu_3\text{-}O)_{12}]^{16+}$ core, comprising a central $[Mn^{IV}{}_4O_4]^{8+}$ cubane held within a non-planar ring of eight Mn^{III} ions by eight μ_3-O^{2-} ions. Peripheral ligation is provided by sixteen η^2-μ-carboxylate groups and four Mn^{III} ions. The eight Mn^{III} ions fall into two groups of four Mn^{III} ions. In group I each Mn^{II} ion is bonded to a single Mn^{IV} *via* two μ_3-O^{2-} bridges, while in group II each Mn^{III} is bonded to two Mn^{IV} ions *via* two μ_3-O^{2-} bridges. The four H_2O ligands coordinate only to Mn^{III} ions in group II.

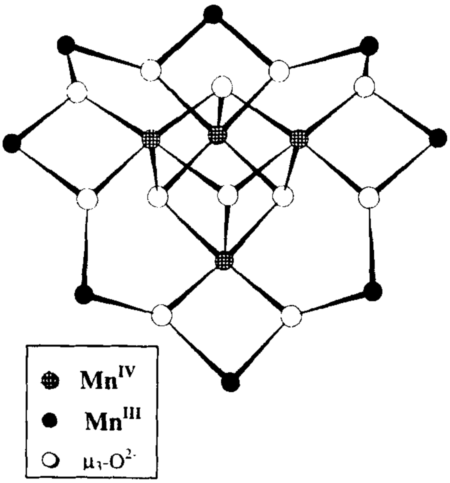

FIGURE 1 Drawing of the $[Mn_{12}(\mu_3\text{-}O)_{12}]^{16+}$ core of a neutral Mn_{12} SMM.

Several new Mn_{12} SMM's have been prepared and structurally characterized. Table I summarizes some of the new complexes, together with those that have already been reported. The X-ray structures of the new complexes will be reported in other

TABLE 1. $[Mn_{12}O_{12}(O_2CR)_{16}(H_2O)_x]\cdot S$ Complexes

R	Isomer	Solvate
$-CH_3$	1,1,1,1	$2HOAc\cdot 4H_2O$
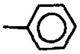	2,2	-
$-CH_2CH_3$	1,1,1	$4\,H_2O$
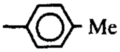	1,1,2	$3\,H_2O$
	1,2,1	$4\,MePhCO_2H$
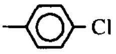	2,2	$8\,CH_2Cl_2$
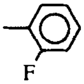	2,2	$4\,CH_2Cl_2\cdot HO_2CC_6H_4\text{-}2F$
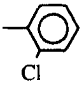	1,2,1	$CH_2Cl_2\cdot 5H_2O$
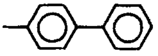	1,1,1,1	-
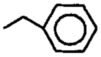	1,2,1	-
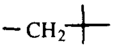	1,2,1	$CH_2Cl_2\cdot CH_3NO_2$

publications. In the case of the p-methylbenzoate complex **6** two different isomers were characterized.[27] Complex **6**$\cdot 3H_2O$ has two H_2O ligands bonded to one Mn^{III} ion and one H_2O ligand on each of two other Mn^{III} ions in group II. Thus, complex **6**$\cdot 3H_2O$ has a (1,1,2) pattern of H_2O ligand positions. The other isomer, complex **6**$\cdot HO_2CC_6H_4\text{-}4Me$, has a (1,2,1) pattern of H_2O ligands. Examination of Table I shows that for the Mn_{12} complexes which have 4 H_2O ligands four different isomeric forms have been identified: (1,1,1,1), (2,1,1), (2,2) and (1,2,1). In Figure 2 are shown drawings of the cores of the different geometric isomers that have been characterized for Mn_{12} SMM's. In total there are eleven possible geometric isomers. The propionate complex **3**, where one Mn atom is five-coordinate, has a (1,1,1) H_2O ligand arrangement. It is interesting that in the case of complex **6**, recrystallization from different solvent media gave two different isomers.

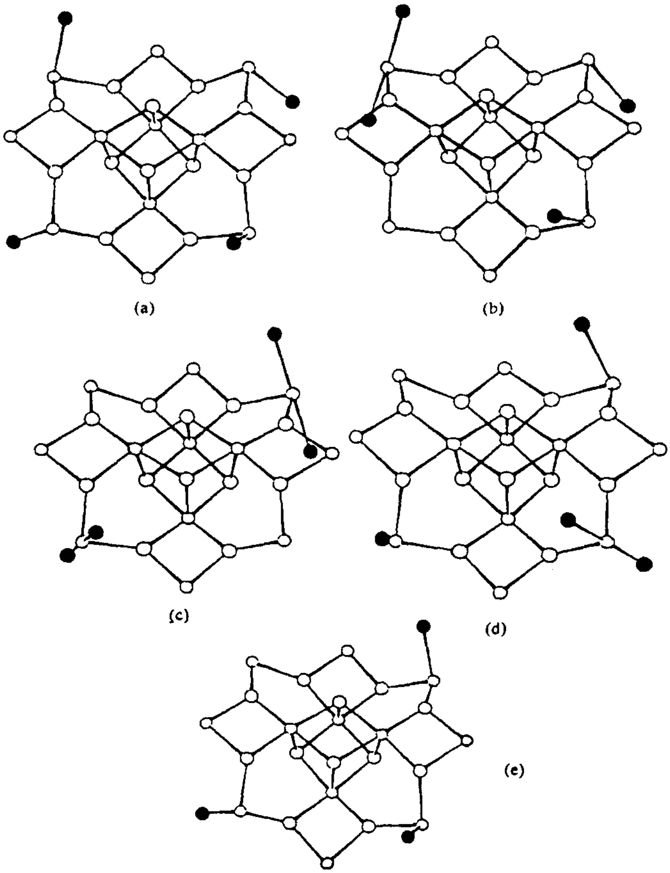

FIGURE 2. Five different geometric isomers of Mn_{12} SMM's found in structurally characterized molecules: (a) (1:1:1:1); (b) (1:1:2); (c) (1:2:1); (d) (2:2); and (e) (1:1:1) isomer.

The two isomers of complex **6** exhibit different ac magnetic susceptibility responses. The observation of a frequency-dependent out-of-phase ac magnetic susceptibility signal in zero dc field is an indication that a molecule functions as a SMM. In the ac susceptibility experiment, the ac magnetic field is oscillated at a particular frequency. An out-of-phase (χ''_M) ac susceptibility signal is observed when the rate at which the magnetic moment of a molecule flips between "up" and "down" is close to the operating frequency of the ac field. Thus, if a sample of a SMM is kept at a certain temperature and the frequency of the ac field is varied, a maximum in the χ''_M signal will occur when the frequency of the field equals the magnetization relaxation rate of the SMM.

χ''_M signals are seen for both **6**·$3H_2O$ and **6**·$HO_2CC_6H_4$-4Me. Figure 3 shows plots (χ''_M *vs*. T) for the two different isomeric forms of complex **6**. Both complexes exhibit two frequency-dependent χ''_M ac peaks, one in the 2-4 K region and the other in the 4-7 K region. However, complex **6**·$HO_2CC_6H_4$-4Me has predominantly a peak in the 2-4 K region, whereas **6**·$3H_2O$ has predominantly a peak in the 4-7 K region.

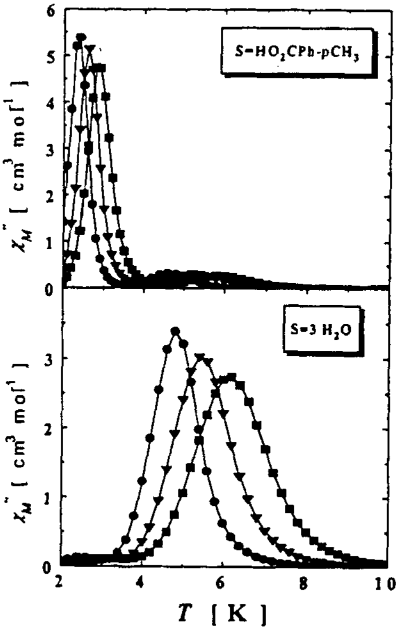

FIGURE 3 Plots of the out-of-phase ac susceptibility χ''_M *vs*. temperature for the two isomers **6**·$HO_2CC_6H_4$-4Me (upper) and **6**·$3H_2O$ (lower). Data were collected with zero dc field and with an 1.0 G ac field oscillating at: (●) 50; (▼) 250 and (■) 1000 Hz.

It has been found that samples of all Mn_{12} SMM's show two χ''_M ac susceptibility signals, one in the 2-4 K region and the other in the 4-7 K region. Even complex **1** shows two χ''_M signals. In the case of certain Mn_{12} SMM's several samples have been made. It has been found that the relative amounts of the two different χ''_M signals change from one sample to another. In fact, in the case of two Mn_{12} SMM's, it was found that there is a time-dependence in the χ''_M signal. Initially complex **7** (R is CH_2Bu^t) shows the 2-4 K peak, but after a few days only a 4-7 K χ''_M peak is seen. In this case it has been established that there is solvate molecule loss than parallels the time dependence in the χ''_M response.

What is the explanation for the appearance of two χ''_M signals for each Mn_{12} SMM? At first it was thought that it was due simply to mixtures of different geometric isomers. However, it is now known that this is not the case. Complexes **7** (R = CH_2Bu^t) and **8** (R = $CH_2C_6H_5$) both have been found to have the (1,2,1) H_2O ligand arrangement. Complex **7** exhibits predominantly the 2-4 K χ''_M peak in agreement with the observations on **6**·$HO_2CC_6H_4$-4Me. However, complex **8** shows predominantly the 4-7 K χ''_M response. Thus, it is not simply the isomeric arrangement of four H_2O and 16 carboxylate ligands that determines the nature of the χ''_M response.

As shown in Figure 4, each Mn_{12} SMM has a double potential-energy well, where the lowest level on the left corresponds to a Mn_{12} molecule with spin "up" and the lowest energy level on the right corresponds to the molecule with spin "down". The diagram is for a SMM with a S = 10 ground state in zero magnetic field. Quantized M_s levels result from zero-field splitting ($D\hat{S}_z^2$) of the S = 10 ground state. For complex **1**, the barrier height is 50 cm^{-1} and it has been shown that when complex **1** is held at temperatuares below 10 K, the complex reverses its direction of magnetization vector by quantum mechanical tunneling through the barrier. This occurs via an Orbach phonon process. A Mn_{12} molecule gets energy from phonons and is excited to a higher-energy level, say the $M_s = -3$ level. It then tunnels through to the $M_s = +3$ level.

There seems to be three possible origins for the two different kinetic barriers seen in the two different χ''_M ac signals for Mn_{12} SMM's. First, the different complexes could have different S and D values for their ground states. There has been some evidence for S = 10 and S = 9 Mn_{12} complexes from variable-field magnetization

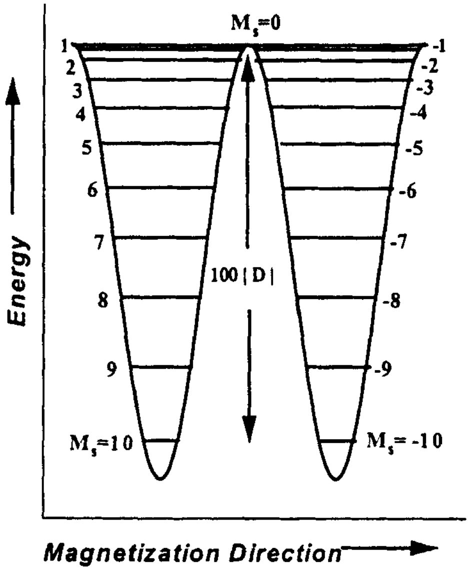

FIGURE 4 Plot of potential energy *vs.* the magnetization direction for a single molecule with a S = 10 ground state split by axial zero-field splitting.

studies. High-field EPR data are needed to check this. The second possible origin for different kinetic barriers lies in different tunneling channels. If two different Mn_{12} complexes have the same S = 10 ground state (see Figure 4), it could be that one complex has a tunneling channel of $M_S = \pm 3$ whereas the other tunnels on the lower-energy $M_S = \pm 4$ levels. The rate of tunneling is determined by transverse magnetic fields (either external or internally within the molecule, as from nuclear spins) or by transverse higher-order zero-field interaction terms. The third possible origin for different kinetic barriers for tunneling in Mn_{12} SMM's lies in the energy ordering of the "spin-ladder" in the different complexes. From one Mn_{12} complex to another, the energy spacing to the first excited spin state may be varying considerable. It is possible that for some Mn_{12} complexes there is a low-energy excited state with a different spin than the ground state. This would introduce a second double well nested on top of the ground-state double well. An Orbach process could excite the Mn_{12} SMM from the M_S = -10 level of the ground state to some level in the excited state double well and the complexes would tunnel with a different effective barrier.

Regardless of the origin of the two different χ''_M peaks for a given Mn_{12} SMM, appreciable differences are also seen in the magnetization hysteresis loops. Figure 5 gives data for the two isomeric forms of complex **6**.

FIGURE 5. Magnetization hysteresis loops measured at 1.90 K for oriented crystals in eicosane matrix for complexes **6**·$3H_2O$ (■) and **6**·$HO_2CC_6H_4$-Me_4 (●). The magnetization for each complex is plotted in units of the saturation magnetization for that complex.

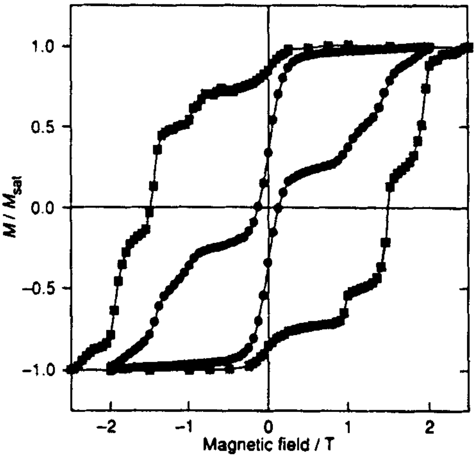

The hysteresis loop of hydrated complex **6**·$3H_2O$ is similar to that reported[16-18] for the acetate complex **1**. On the other hand, complex **6**·$HO_2CC_6H_4$-4Me shows a much steeper step at zero field than does complex **6**·$3H_2O$. Thus, complex **6**·$HO_2CC_6H_4$-4Me is exhibiting an appreciably faster rate of tunneling of the magnetization than the other isomer. This is the case in spite of the fact that both forms of complex **6** have the same ligands and only differ in their arrangements of four H_2O ligands and space groups. The greater rate of tunneling for complex **6**·$HO_2CC_6H_4$-4Me is consistent with the fact that this complex shows its χ''_M ac signal at a lower temperature than does the hydrated complex **6**. It will take additional research to determine the origin(s) of the different rates of quantum tunneling of magnetization.

$[\text{Cation}][Mn_{12}O_{12}(O_2CR)_{16}(H_2O)_4]$ SMM's.

The feasibility of chemically reducing a Mn_{12} SMM was established by the observation of a reversible one-electron reduction process in the cyclic voltammogram of a solution containing complex **3**. The salt $(PPh_4)[Mn_{12}O_{12}(O_2CEt)_{16}(H_2O)_4]$ (**9**) was first reported[4a] in 1995 and the presence of steps in the magnetization hysteresis loops was communicated.[29] Very recently, a reduced salt with an organic radical cation, (m-$MPYNN^+)[Mn_{12}O_{12}(O_2CPh)_{16}(H_2O)_4^-]$, was reported,[30] where m-$MPYNN^+$ is m-N-methylpyridinium nitronylnitroxide.

The $[Mn_{12}]^-$ anions in complex **9** have been shown[4a] with magnetization *vs.* magnetic field data to have a S = 19/2 ground state. This has been confirmed[31] by high-field EPR spectra that also give an accurate value for the zero-field splitting parameter D = -0.61 cm^{-1}. The double-well potential energy diagram for a S = 19/2 SMM with *negative* magnetoanisotropy is shown in Figure 6. The double well represents the change in potential energy of one $[Mn_{12}^-]$ anion in zero field as the anion changes the direction of its magnetic moment. Again there are quantized levels

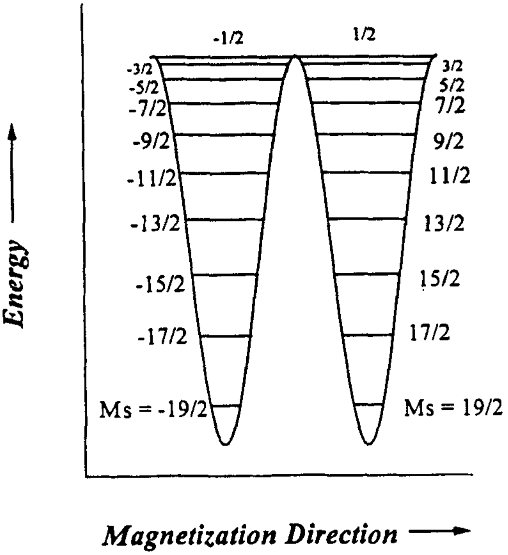

FIGURE 6. Plot of potential energy *vs.* the magnetization direction for a single molecule with a S = 19/2 ground state.

as a result of the zero-field splitting. One of the most important questions about these $[Mn_{12}^{-}]$ complexes is whether they will show resonant quantum tunneling. In zero magnetic field a half-integer SMM should not be able to tunnel coherently.[32]

The rate of relaxation of the magnetization was measured for a polycrystalline sample of complex **9** equilibrated at one of five temperatures in the range 1.8-2.5 K in an external magnetic field of 3.5 T; the latter was then quenched to zero. The decrease in magnetization measured at each temperature was fitted to a distribution of single exponentials to give the relaxation rate. Relaxation rates were also determined in the range of 3.2-7.2 K by means of ac magnetic susceptibility measurements in zero dc field. At a fixed temperature, the in-phase (χ'_M) and out-of-phase (χ''_M) components of magnetic susceptibility were measured as the frequency of the ac field (0.05 Oe) was varied from 0.01 to 1500 Hz. The relaxation time (τ) at a given temperature was determined by fitting the data to eqn. (1), where ω is angular frequency ($2\pi\nu$), χ_S is the

$$\chi'_M = \chi_S + (\chi_T - \chi_S)/(1 + \omega^2\tau^2) \qquad (1)$$

adiabatic susceptibility (*i.e.*, $\omega \rightarrow 0$) and χ_T is the isothermal (susceptibility (*i.e.*, $\omega \rightarrow 0$)). The relaxation rates varied from $3.94 \times 10^4\ s^{-1}$ at 7.2 K to $6.19 \times 10^{-6}\ s^{-1}$ at 1.8 K. Figure 7 shows an Arrhenius plot of $\ln(1/\tau)$ *versus* $1/T$. These data were fit to the Arrhenius law to give a barrier height, U, of 60.2 K with an preexponential ($1/\tau_0$) of $1.31 \times 10^8\ s^{-1}$. This is compared with U = 61-67 K and $1/\tau_0 \approx 10^7\ s^{-1}$ found[20] for the S = 10 molecule Mn_{12}-acetate (complex **1**).

In Figure 8 is shown the magnetization hysteresis loop taken at 1.85 K for an oriented-crystal sample of complex **9**. The magnetic field was applied along the easy axis of the oriented crystals. The sample was first saturated in a field of +2.0 T, and the field then swept down to -2.0 T, and cycled back to +2.0 T. The sweep rate was 25 Oe/s. Steps can clearly be seen on the hysteresis loop. In the lower part of Figure 8 is shown the first derivative of the hysteresis plot. As the field is decreased from +2.0 T, the first step is seen at zero field, followed by steps at -0.4686, -0.9022, and -1.262 T. The steps correspond to increases in the rate of change of the magnetization, and are due to resonant tunneling between quantum spin states. Thus, as the magnetic field is varied, levels in the two halves of the double well shown in Figure 6 have the same energy at certain field values. When energy levels line up, one in the left part of the double well and the other in the right part, resonant tunneling of the magnetization occurs.

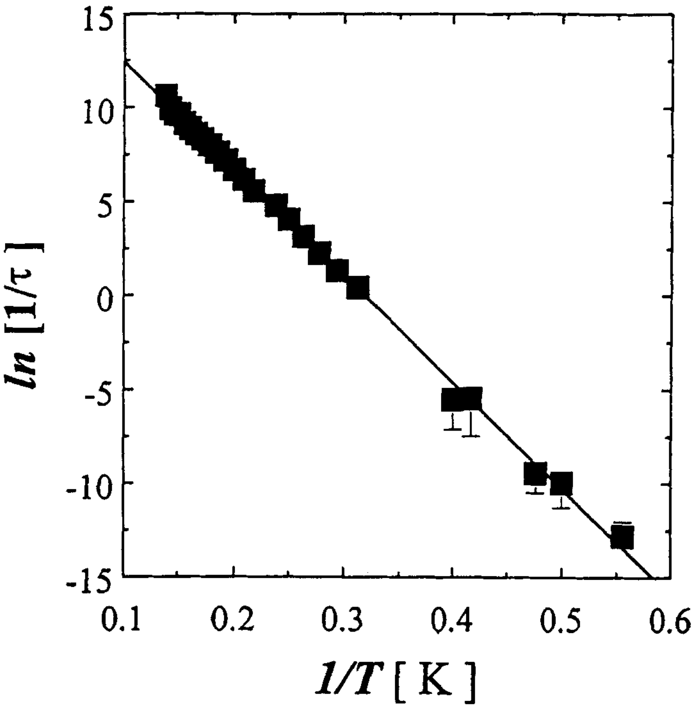

FIGURE 7. Plot of the logarithm of the rate of relaxation *vs.* the inverse absolute temperature for $(PPh_4)[Mn_{12}O_{12}(O_2CEt)_{16}(H_2O)_4]$ (**9**).

There have been several papers[32] addressing the fact that a molecule with an half-integer ground state, such as S = 19/2, should not exhibit resonant tunneling in the absence of a magnetic field. For such a molecule, each pair of $\pm M_S$ levels in zero-field constitutes a Kramers degeneracy. However, from Figure 8 it is clear that complex **9** shows a step in its hysteresis loop at zero external magnetic field. This S = 19/2 complex tunnels not only at various increments of field, but also when H = 0. This is very probably due to the fact there is an internal magnetic field within the $[Mn_{12}^-]$ complex. The ^{55}Mn and ^1H nuclei have spins of I = 5/2 and I = 1/2, respectively,

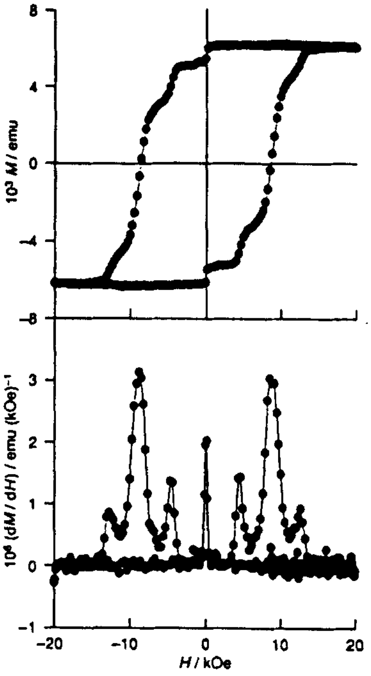

FIGURE 8. The top plot shows the magnetization hysteresis loop measured at 1.85 K for five crystals of $(PPh_4)[Mn_{12}O_{12}(O_2CEt)_{16}(H_2O)_4]$ oriented in an eicosane wax matrix. In the lower plot is shown the first derivative of the magnetization hysteresis loop.

and this will give rise to a small internal magnetic field (10-200 Oe) in the molecule. A transverse component of this internal magnetic field breaks the symmetry in each $\pm M_s$ Kramers pair and leads to resonant tunneling of the magnetization.

The $[Mn_4O_3Cl(O_2CCH_3)_3(dbm)_3]$ SMM

Distorted cubane complexes with a $[\mathrm{Mn^{IV}Mn^{III}_3O_3X}]^{6+}$ core have been shown[33] to exhibit frequency-dependent out-of-phase ac susceptibility signals. These Mn_4 complexes are also SMM's. It has been well established that all of these complexes have S = 9/2 ground states employing variable-field magnetization data.[34] HFEPR data[35] for $[Mn_4O_3Cl(O_2CCH_3)_3(dbm)_3]$ (**10**) confirm that this complex has a S = 9/2 ground state, split by zero-field splitting with D = -0.53 cm^{-1} ($D\hat{S}_z^2$) and B_4^0 = 7.3 x 10^{-5} cm^{-1} ($B_4^0\hat{O}_4^0$). The ligand dbm$^-$ is the anion of dibenzoylmethane.

Two very exciting observations were made for complex **10**.[35,36] First, it was found that steps are seen in the magnetization hysteresis loops for complex **10**. Second, complex **10** shows a temperature-independent rate of magnetization relaxation below 0.6 K. This $S = 9/2$ SMM exhibits a tunneling of its direction of magnetization at a rate of $3.2 \times 10^{-2}\ s^{-1}$ in the 0.394-0.600 K range.

Magnetization data were obtained for a plate-like ~1 x 1 x 0.1 mm single crystal of complex **10** at five different temperatures between 0.426 and 2.21 K employing a Faraday magnetometer equipped with a ^3He refrigerator. The single crystal was oriented and fixed in a solid eicosane cube with the external field parallel to the magnetization easy axis of the crystal. After saturation (+2.0 T) the field was cycled between +2.0 T and -2.0 T and back to +2.0 T. No hysteresis loop was seen at 2.21 K. The data at the other four temperatures are shown in Figure 9. Steps are clearly seen in these hysteresis loops. At 0.426 K, as the field is decreased from 2.0 T to -2.0 T, a large step is seen at zero field, with a less pronounced step seen at -0.55 T.

The steps are attributable to resonant tunneling between quantum levels. The spacings between the steps seen in the hysteresis loop are given by $\Delta H = -D/g\mu_B$, where g is the EPR g-factor and μ_B is the Bohr magneton. The parameter D gauges the magnitude of axial zero-field splitting ($D\hat{S}_z^2$) present in the $S = 9/2$ ground state of complex **10**. From the first-derivative plot in Figure 9, the average field interval between steps is calculated to be $\Delta H = 0.55$ T. This gives a value of $D/g = -0.25\ cm^{-1}$, which is consistent with the $D/g = -0.18\ cm^{-1}$ obtained for this compound by fitting variable-field magnetization data[34] and also with fitting of high field EPR data ($D/g = -0.25\ cm^{-1}$).[35]

Rates of magnetization relaxation for complex **10** have been determined in the 1.7 - 2.1 K range by means of ac susceptibility measurements and in the 0.394 - 0.706 K range with the Faraday magnetometer. In the case of the ac susceptibility experiment, the frequency of the ac field is held fixed. The frequency of the ac field corresponds to the rate of magnetization relaxation at the temperature at which there is a maximum in the out-of-phase ac signal. In the low temperature range rates of magnetization were determined by saturating the magnetization of a single crystal in the Faraday balance. After the field was rapidly decreased to zero, the decay of the magnetization for the crystal was measured as a function of time. These relaxation data were fit as an exponential decay to give the relaxation rate of each temperature in the 0.394 - 0.706 K

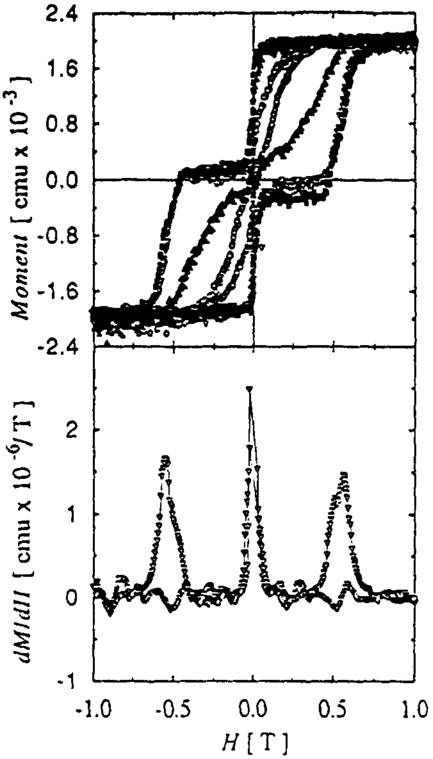

FIGURE 9. (Top) Magnetization hysteresis loops measured for a single crystal of complex **10** at the following temperatures: (■) 0426 K; (▼) 0.530 K; (▲) 0.706 K; and (○) 0.900 K. One complete hysteresis loop took 48 min and was measured in the 2.0 to -2.0 T range. (Bottom) First derivative of the loop measured at 0.530 K.

range. An Arrhenius plot of ln(rate) *vs.* 1/T (Figure 10) shows an activated higher temperature region with a barrier of ~12 K and a preexponential factor of 4 x 10^{-7} s. At the lowest temperature (< 0.706 K), the relaxation rate becomes independent of temperature with a tunneling rate equal to 3 x 10^{-2} s^{-1}.

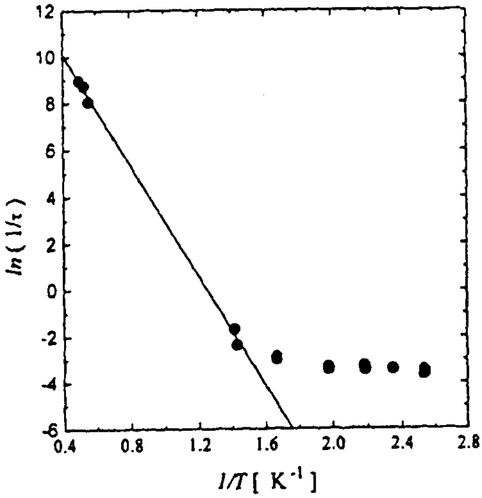

FIGURE 10. Plot of the natural logarithm of the rate of magnetization relaxation (1/τ) *versus* the inverse of the temperature for complex **10**. The line is a least-squares fit of the higher temperature data to the Arrhenius equation.

The temperature-independent magnetization tunneling rate of 3.2 x 10^{-2} s^{-1} determined for complex **10** in the 0.394-0.600 K range must be due to tunneling between the M_S = 9/2 and +9/2 levels of the S = 9/2 ground state. This is in contrast to what has been found for the M_{12}-Ac complex **1**. In that case the tunneling rates for the lowest levels are too slow. It has been calculated that the lifetime for tunneling between the M_S = -10 and M_S = +10 levels of the S = 10 ground state is longer than the lifetime of the universe. Presumably the Mn_{12} complex **1** is excited to higher M_S levels via a multiphonon Orbach process. Complex **1** may tunnel via higher levels such as the M_S = ±3 levels (see Figure 4).

CONCLUDING COMMENTS

Several different types of single-molecule magnets have been characterized. Considerable work needs still to be done to understand the mechanism of the resonant magnetization tunneling that is seen. What roles do internal transverse magnetic fields or higher-order zero-field effects play in determining the rate of tunneling? It is an important challenge to increase the barrier for magnetization relaxation in these SMM's. This will require molecules with both larger spin ground states as well as greater magnetoanisotropy. Another significant goal is the preparation of ordered arrays of SMM's to begin the study of their utilization as memory devices.

ACKNOWLEDGMENTS

This work was supported by the National Science Foundation (G.C. and D.N.H.) and the Department of Energy under Grant No. DE-FG03-86ER-45230 (M.B.M.). The ac magnetic susceptibility measurements were performed with a MPMS2 SQUID magnetometer provided by the Center for Interface and Material Science, funded by the W. M. Keck Foundation.

References

[1] L. Gunther, *Physics World*, December 28 (1990).

[2] (a) G.P. Berman, G.D. Doolen, D.D. Holm and V.I. Tsifrinovich, *Physics Lett. A 193*, 444 (1994). (b) D.A. Garanin and E.M. Chudnovsky, *Phys. Rev. B.*, **56,** 11102 (1997).

[3] (a) D.D. Awschalom and D.P. Di Vincenzo, *Physics Today*, **48** 43 (1995). (b) D.L. Leslie-Pelecky and R.D. Rieke, *Chem. Mater.*, **8** 1770 (1995). (c) L. Gunther, *Physics World*, December 28 (1990). (d) D.D. Awschalom, D.P. Di Vincenzo and J.F. Smyth, *Science*, **258** 414 (1992). (e) P.C.E. Stamp, E. M. Chudnosvsky and B. Barbara, *Int. J. Mod. Phys.*, **B6** 1355 (1992). (f) S. Gider, D.D. Awschalom, T. Douglas, S. Mann and M. Chaparala, ***Science*,268**, 77 (1995).

[4] (a) H.J. Eppley, H.-L. Tsai, N. de Vries, K. Folting, G. Christou and D.N. Hendrickson, *J. Am. Chem. Soc.*, **117** 301 (1995). (b) S.M.J. Aubin, H.J. Eppley, I.A. Guzei, K. Folting, P.K. Gantzel, A.L. Rheingold, G. Christou and D.N. Hendrickson, submitted for publication. (c) M.A. Novak, R. Sessoli, A. Caneschi and D. Gatteschi, *J. Magn. Magn. Mater.*, **146,** 211 (1995). (d) M. Sorai, H.J. Eppley, S.M.J. Aubin, G. Christou and D.N. Hendrickson, unpublished results.

[5] R. Sessoli, *Mol. Cryst. Liq. Cryst.* **274**, 145 (1995).

[6] T. Lis, *Acta Cryst* **B36** 2042 (1980).

[7] R. Sessoli, D. Gatteschi, A. Caneschi and M. A. Novak, *Nature 365, 141*(1993).

[8] D. Gatteschi, A. Caneschi, L. Pardi and R. Sessoli, *Science, 265* 1054 (1994).

[9] P. D. W. Boyd, Q. Li, J. B. Vincent, K. Folting,H.-R. Chang, W. E. Streib, J. C. Huffman, G. Christou and D. N. Hendrickson, *J. Am. Chem. Soc. 110*8537 (1988).

[10] A. L. Barra, A. Caneschi, D. Gatteschi and R. Sessoli, *J. Am. Chem. Soc. 117*, 885 (1995).

[11] E. M. Chudnovsky, *Science, 274,* 938 (1996).

[12] M. A. Novak, and R. Sessoli, in *Ouantum Tunneling of Magnetization-QTM'94,*edited by L. Gunther and B. Barbara, (Kluwer Academic Publishers: Dordrecht, 1995), pp 171–188.

[13] C. Paulsen and J.-G. Park, in *Quantum Tunneling of Magnetization-QTM'94,*edited by L. Gunther and B. Barbara, (Kluwer Academic Publishers: Dordrecht, 1995), pp 189–207.

[14] R. Politi, A. Rettori, F. Hartmann-Boutron and J. Villain, *Phys. Rev. Lett., 75,*537 (1995).

[15] J. M. Hernandez, JX. X. Zhang, F. Luis, J. Bartolomé, J. Tejada and R. Ziolo, *Europhys. Lett. 35* 301 (1996).

[16] (a) J. R. Friedman, M. P. Sarachik, J. Tejada, J. Maciejewski and R. Ziolo, *J. Appl. Phys., 79,* 6031 (1996). (b) J. R. Friedman, M. P. Sarachik, J. Tejada and R. Ziolo, *Phys. Rev. Lett., 76,* 3830 (1996). (c) J. R. Friedman, Ph.D. Thesis, 1996, The City College of New York, New York City, NY.

[17] L. Thomas, F. Lionti, R. Ballou, D. Gatteschi, R. Sessoli and B. Barbara, *Nature, 383,* 145 (1996).

[18] J. Tejada, R. F. Ziolo and X. X. Zhang, *Chem. Mater.* 8, 1784 (1996).

[19] B. Schwarzschild, *Phys. Today,* January 17 (1997).

[20] F. Lionti, L. Thomas, R. Ballou, B. Barbara, A. Sulpice, R. Sessoli and D. Gatteschi *J. Appl.*81 4608 (1997).

[21] J. R. Friedman, M. P. Sarachik, J. M. Hernandez, X. X. Zhang, J. Tejada, E. Molins and R. Ziolo, *J. Appl. Phys., 81,* 3978 (1997).

[22] A. L. Barra,D. Gatteschi and R. Sessoli, *Phys. Rev. B, 56,* 8192 (1997).

[23] F. Luis, J. Bartolomé and J. F. Fernández, *Phys. Rev. B, 55,* 11448 (1997).

[24] J. M. Hernandez, X., X. Zhang, F. Luis, J. Tejada, J. R. Friedman, M. P. Sarachik and R. Ziolo, *Phys. Rev. B, 55,* 5858 (1997).

[25] F. Luis, J. Bartolomé, J. F. Fernández, *Phys. Rev. B, 56,* 11102 (1997).

[26] R. Sessoli, H.-L. Tsai, A. R. Schake, S. Wang, J. B. Vincent, K. Folting, D. Gatteschi, G. Christou and D. N. Hendrickson, *J. Am. Chem. Soc., 115,* 1804 (1993).

[27] D. Ruiz, Z. Sun, B. Albela, K. Folting, J. Ribas, G. Christou, and D. N. Hendrickson, *Angew. Chem. Int. Ed., 37,* 300 (1998).

[28] S. M. J. Aubin, Z. Sun, I. A. Guzei, A. L. Rheingold, G. Christou, and D. N. Hendrickson, *Chem. Commun.,* 2239 (1997).

[29] S. M. J. Aubin, S. Spagna, H. J. Eppley, R. E. Sager, G. Christou, and D. N. Hendrickson, *Chem. Commun.,* 803 (1998).

[30] K. Takeda and K. Awaga, *Phys. Rev B. 56,* 14560 (1997).

[31] S. M. J. Aubin, Z. Sun, L. Pardi, J. Krzystek, K. Folting, L.-C. Brunel, A. L. Rheingold, G. Christou and D. N. Hendrickson, submitted for publication.

[32] (a) D. Loss, D. P. Di Vincenzo, G. Grinstein, D. Awschalom and J. F. Smyth, *Physica B,* 189, 189 (1993). (b) D. P. Di Vincenzo, *Physica B, 197,* 109 (1994).

[33] S. M. J. Aubin, M. W. Wemple, D. M. Adams, H.-L. Tsai, G. Christou, and D. N. Hendrickson, *J. Am. Chem. Soc., 118,* 7746 (1996).

[34] D. N. Hendrickson, G. Christou, E. A. Schmitt, E. Libby, J. S. Bashkin, S. Wang, H.-L. Tsai, J. B. Vincent, P. D. W. Boyd, J. C. Huffman, K. Folting, Q. Li, and W. E. Streib, *J. Am. Chem. Soc., 114,* 2455 (1992).

[35] S. M. J. Aubin, N. R. Dilley, L. Pardi, J. Krzystek, M. V. Wemple, L.-C. Brunel, M. B. Maple, G. Christou and D. N. Hendrickson, *J. Am. Chem. Soc., 120* 4991 (1998).

[36] S. M. J. Aubin, N. R. Dilley, M. W. Wemple, M. B. Maple, G. Christou, and D. N. Hendrickson, *J. Am. Chem. Soc., 120,* 839 (1998).